

MAGNETIC FIELDS IN STARBURST GALAXIES AND THE ORIGIN OF THE FIR-RADIO CORRELATION

TODD A. THOMPSON,^{1,2} ELIOT QUATAERT,³ ELI WAXMAN,⁴ NORMAN MURRAY,^{5,6} & CRYSTAL L. MARTIN⁷

SUBMITTED TO APJ: JANUARY 26, 2006

ABSTRACT

We estimate minimum energy magnetic fields (B_{\min}) for a sample of galaxies with measured gas surface densities. The sample spans more than four orders of magnitude in surface density from normal spirals to luminous starbursts. We show that the ratio of the minimum energy magnetic pressure to the total pressure in the ISM decreases substantially with increasing surface density. For the ultra-luminous infrared galaxy Arp 220, this ratio is $\sim 10^{-4}$. Therefore, if the minimum energy estimate is applicable, magnetic fields in starbursts are dynamically weak compared to gravity, in contrast to our Galaxy and other normal star-forming spiral galaxies. We argue, however, that rapid cooling of relativistic electrons in starbursts invalidates the minimum energy estimate. We critically assess a number of independent constraints on the magnetic field strength in starburst galaxies. In particular, we argue that the existence of the FIR-radio correlation implies that the synchrotron cooling timescale for cosmic ray electrons is much shorter than their escape time from the galactic disk; this in turn implies that the true magnetic field in starbursts is significantly larger than B_{\min} . The strongest argument *against* such large fields is that one might expect starbursts to have steep radio spectra indicative of strong synchrotron cooling, which is not observed. We show, however, that ionization and bremsstrahlung losses can flatten the nonthermal spectra of starburst galaxies even in the presence of rapid cooling, providing much better agreement with observed spectra. We further demonstrate that ionization and bremsstrahlung losses are likely to be important in shaping the radio spectra of most starbursts at GHz frequencies, thereby preserving the linearity of the FIR-radio correlation. We thus conclude that magnetic fields in starbursts are significantly larger than B_{\min} . We highlight several observations that can test this conclusion.

Subject headings: galaxies:general — galaxies:magnetic fields — galaxies:starburst — infrared:galaxies — radio continuum:galaxies

1. INTRODUCTION

The magnetic energy density of the Galaxy is observed to be in rough equipartition with the cosmic ray energy density and the turbulent pressure. The sum of these yields a total midplane pressure consistent with that required by hydrostatic equilibrium, given the mass distribution in the solar neighborhood (Boulares & Cox 1990). This equipartition magnetic field is roughly $6 \mu\text{G}$ at the solar circle (e.g., Beck 2001). Similar magnetic field strengths are found in most normal star-forming spiral galaxies (Fitt & Alexander 1993; Niklas 1995).

Starbursts and ultra-luminous infrared galaxies (ULIRGs) have much higher surface densities and turbulent velocities than local spirals. As an example, Arp 220 has a gas surface density $\sim 10^4$ times higher than the Galaxy (Downes & Solomon 1998). If Arp 220 has a magnetic energy density in rough equipartition with its hydrostatic pressure, the

implied magnetic field strength would be $\sim 0.03\text{G}$ on few-hundred parsec scales (Fig. 1, Table 2). This is substantially larger than the value of $\sim 1\text{mG}$ typically inferred in ULIRGs (e.g., Condon et al. 1991) using the observed radio emission and the classic “minimum energy” argument (Burbidge 1956; Longair 1994).

Throughout this paper we use the term “minimum energy” to refer to the magnetic field strength inferred using the observed radio flux and assuming comparable cosmic ray and magnetic energy densities (B_{\min} ; eq. [1]). We reserve the term “equipartition” for magnetic field strengths that are dynamically important with respect to gravity (B_{eq} ; eq. [3]).

We find that the large discrepancy between the minimum energy and equipartition magnetic field estimates in Arp 220 is generic to starburst galaxies; this discrepancy motivates the analysis of magnetic field strengths in luminous starbursts presented in this paper. In §2 we present a sample of galaxies with measured gas surface densities and radio fluxes, for which both minimum energy and equipartition field strengths can be estimated. In §3 we summarize arguments in favor of $B \sim B_{\min}$ and against significantly larger fields. Rebuttals to a subset of these arguments are given in §4, where we also provide independent arguments why magnetic fields in starbursts are likely to be $\gg B_{\min}$. These arguments draw heavily on the FIR-radio correlation for star-forming galaxies and the observed radio spectra of starbursts. Finally, in §5 we summarize our results and discuss their implications.

¹ Department of Astrophysical Sciences, Peyton Hall-Ivy Lane, Princeton University, Princeton, NJ 08544; thomp@astro.princeton.edu

² Lyman Spitzer Jr. Fellow

³ Astronomy Department & Theoretical Astrophysics Center, 601 Campbell Hall, The University of California, Berkeley, CA 94720; eliot@astro.berkeley.edu

⁴ Physics Faculty, Weizmann Institute of Science, Rehovot 76100, Israel; waxman@wicc.weizmann.ac.il

⁵ Canada Research Chair in Astrophysics

⁶ Canadian Institute for Theoretical Astrophysics, 60 St. George Street, University of Toronto, Toronto, ON M5S 3H8, Canada; murray@cita.utoronto.ca

⁷ Department of Physics, The University of California, Santa Barbara, CA 93106; cmartin@physics.ucsb.edu

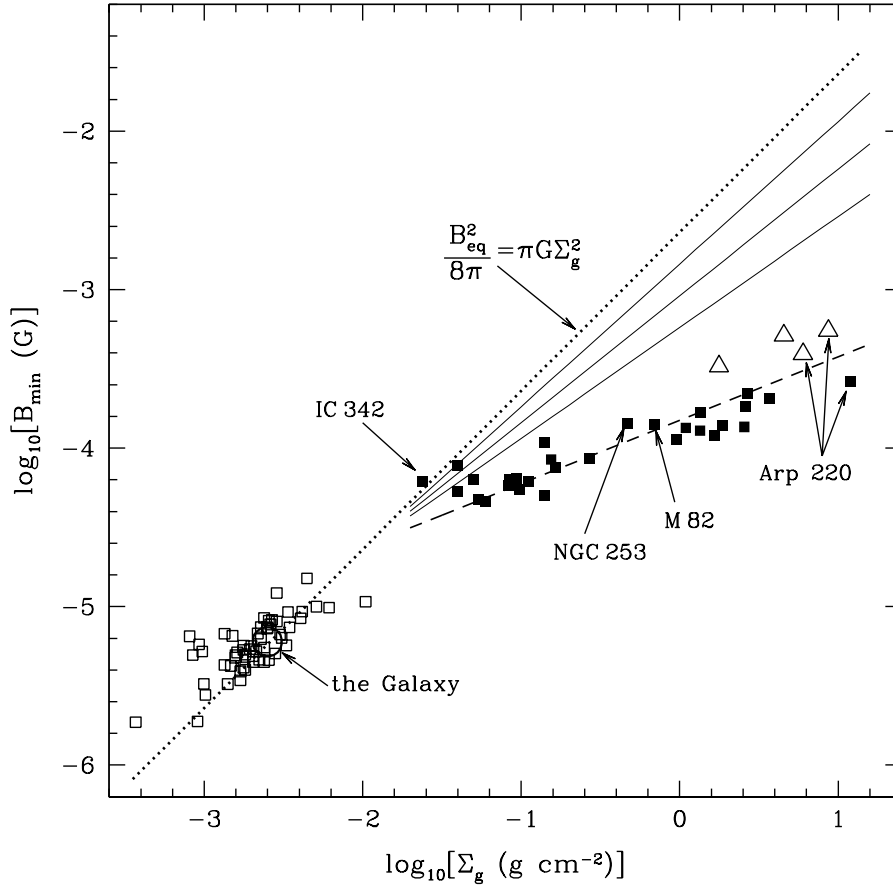


FIG. 1.— Minimum energy magnetic field (B_{\min} ; eq. [1]) versus measured gas surface density (Σ_g). Normal star-forming galaxies (open squares; Table 1), starburst galaxies (filled squares; Table 2), and the Galaxy ($B_{\min} = 6 \mu\text{G}$ at the solar circle, e.g., Beck 2001; $\Sigma_g \simeq 2.5 \times 10^{-3} \text{ g cm}^{-2}$, Boulares & Cox 1990) are shown. To indicate the uncertainties at high Σ_g , the open triangles show B_{\min} for IC 883 (Arp 193), Mrk 273, and the individual nuclei of Arp 220, as inferred using Σ_g and the radial size from Downes & Solomon (1998) (their “extreme” starbursts; see their Table 12) and with the radio flux from Condon et al. (1991) at 8.44 GHz (see Table 3). The dotted line is the equipartition magnetic field (eq. [3]) and the dashed line is the scaling $B_{\min} \propto \Sigma_g^{2/5}$ (eq. [11]). The latter scaling is expected if the cosmic ray electron cooling timescale is much shorter than the escape timescale from the galactic disk, in which case the true magnetic field is also significantly larger than the minimum energy estimate (see §4; eq. [11]). The solid lines show the scalings $B \propto \Sigma_g^a$ (with $a = 0.9, 0.8,$ and 0.7) used in §4.3.

2. DATA & RESULTS

Longair (1994) derives the minimum energy magnetic field strength as (Vol. II, eq. [19.30])

$$B_{\min} \approx 7 \times 10^{-4} \delta_2^{2/7} L_{\nu,23}^{2/7} V_6^{-2/7} \nu_{\text{GHz}}^{1/7} \text{ G} \quad (1)$$

where $L_{\nu,23} = L_{\nu}/10^{23} \text{ W Hz}^{-1}$, $\nu_{\text{GHz}} = \nu/10^9 \text{ Hz}$, $V_6 = V/(100)^3 \text{ pc}^3$ is the volume of the emitting region, $\delta_2 = \delta/10^2$ is the ratio of the energy in cosmic ray ions to the energy in cosmic ray electrons, and the derivation assumes that the cosmic ray electron energy spectrum is $n(\gamma) \propto \gamma^{-p}$ with $p = 2.5$. We have scaled the results above for parameters appropriate to compact starbursts. For parameters typical of the Galaxy, $L_{\nu,23} \sim 3 \times 10^{-2}$ and $V_6 \sim 7 \times 10^4$ so that $B_{\min} \approx 10^{-5} \text{ G}$.

The minimum energy magnetic field strength is often referred to as “equipartition” because the corresponding magnetic energy density ($U_{B_{\min}}$) is approximately equal to the total cosmic ray (electron + ion) energy density if B_{\min} actually obtains. In this paper, however, we use the term “equipartition” to denote magnetic energy densities comparable to the total hydrostatic pressure of the ISM. For a gas disk of sur-

face density Σ_g , hydrostatic equilibrium with the self-gravity of the disk implies a midplane pressure

$$P \approx \pi G \Sigma_g^2. \quad (2)$$

We measure equipartition via the parameter η defined by $U_B = \eta P$. The equipartition ($\eta = 1$) field strength is thus

$$B_{\text{eq}} \approx (8\pi^2 G)^{1/2} \Sigma_g \approx 2 \Sigma_g \text{ mG}, \quad (3)$$

where Σ_g is in cgs units. Theoretically, there are significant uncertainties about the origin of magnetic fields in galactic disks, and so it is difficult to estimate the expected value of η . Field strengths as large as equipartition are, however, possible if the magnetic energy density equilibrates with the turbulent energy density of the ISM. The scale-height h of a self-gravitating galactic disk is given by $h \sim \delta v^2 / 2\pi G \Sigma_g$, where δv is the turbulent velocity. As a result, the energy density in turbulent motions is $\rho \delta v^2 \sim \pi G \Sigma_g^2$, where ρ is the mean density of the ISM. Thus, if the field is amplified by the turbulent motions so that $B^2 / 8\pi \sim \rho \delta v^2$, equipartition follows.

The gravitational potential of normal star-forming galaxies includes a significant contribution from stars (and per-

haps dark matter) on the scale of their effective radii. Neglecting for simplicity the different scale-heights of stars and gas, equation (2) should then be replaced by $P \approx \pi G \Sigma_g \Sigma_{\text{tot}} \approx \pi G \Sigma_g^2 f_g^{-1}$, where f_g is the gas fraction and Σ_{tot} is the total surface density. Typically, f_g is in the range $\sim 0.1 - 0.2$ for normal galaxies and $f_g \sim 0.5$ for starbursts. Thus, the magnetic field could in principle be larger than equation (3) by a factor of $f_g^{-1/2}$ and still be sub-dominant with respect to gravity. In this paper, these distinctions are not important because we focus on gas-rich starbursts and use equation (3) primarily as a useful point of comparison for field strengths inferred using the minimum energy argument (eq. [1]).

Figure 1 shows the minimum energy magnetic field B_{min} inferred using equation (1) as a function of the surface density Σ_g of the galactic disk for a sample of galaxies ranging from local spirals to ULIRGs. The sample is based on galaxies with surface densities and sizes used by Kennicutt (1998) to study the global properties of star formation across a range of galaxies (the ‘‘Schmidt Laws’’). The properties of the normal star-forming and starburst galaxies are listed in Tables 1 and 2, respectively. Systems described as starbursts by Kennicutt are denoted here by solid squares, whereas his normal star-forming galaxies are labeled by open squares.

In computing the radio emitting volume (eq. [1]), we assume that the scale height of the synchrotron emission is $h_{\text{rad}} = 500$ pc for the normal galaxies (Beuermann et al. 1985; Dumke & Krause 1998) and $h_{\text{rad}} = 100$ pc for the starbursts (filled squares) (e.g., Klein et al. 1988; Seaquist & Odegard 1991; Condon et al. 1991).⁸ We use radial sizes from Kennicutt (1998); for normal galaxies, these are taken from the RC2 catalog (de Vaucouleurs et al. 1976). Detailed studies show that for spiral galaxies the ratio of the optical to radio disk scale length is $\sim 0.9 - 1.3$ (Hummel 1980; Fitt & Alexander 1993). For both the normal galaxies (open squares) and the starbursts (filled squares), we have computed B_{min} using the radio luminosity at 1.4 GHz.

The open triangles illustrate the uncertainties in the results of Figure 1 at high Σ_g . These points denote the ‘‘extreme’’ starbursts of Downes & Solomon (1998) (see their Table 12): IC 883 (Arp 193), Mrk 273, and the two individual nuclei of Arp 220. For these systems, we use the gas surface densities and radial sizes from Downes & Solomon (instead of Kennicutt 1998), and we combine this data with radio fluxes from the 8.44 GHz observations of Condon et al. (1991), which have sufficient resolution to probe the same spatial scales as the observations of Downes & Solomon (in contrast to the 1.4 GHz observations used for the rest of the systems in Fig. 1). The properties of these starbursts are collected in Table 3. Although the inferred B_{min} is somewhat larger at a given Σ_g than for the starburst sample in Table 2 (filled squares in Fig. 1), the reasonably close correspondence is encouraging.

In addition to the inferred minimum energy magnetic field, Figure 1 also includes several theoretical curves. The dotted line shows the equipartition magnetic field (eq. [3]) while the dashed line shows the scaling $B_{\text{min}} \propto \Sigma_g^{2/5}$ derived in §4.1. Finally, the solid lines show the scalings $B \propto \Sigma_g^a$ (with $a = 0.9, 0.8, \text{ and } 0.7$) used in our discussion of the FIR-radio correlation in §4.3. Although these alternative (non-equipartition) scalings are somewhat arbitrary, the particular choice $B \propto \Sigma_g^{0.7}$

⁸ $B_{\text{min}} \propto h_{\text{rad}}^{-2/7}$ so uncertainties in h_{rad} introduce only modest uncertainties in B_{min} .

is physically motivated by setting the magnetic energy density equal to the pressure in the ISM produced by star formation (P_*). Because $P_* \propto \dot{\Sigma}_*$ (where $\dot{\Sigma}_*$ is the star formation rate per unit area; see, e.g., Chevalier & Clegg 1985, Thompson, Quataert, & Murray 2005) and because the Schmidt law for star formation is $\dot{\Sigma}_* \propto \Sigma_g^{1.4}$ (Kennicutt 1998), the scaling $B \propto \Sigma_g^{0.7}$ follows.

Our estimates of B_{min} in Figure 1 for normal star-forming galaxies are in good agreement with those estimated by other authors (e.g., Fitt & Alexander 1993; Niklas 1995; Beck 2000). When these minimum energy fields can be compared with other magnetic field estimates (e.g., from Faraday rotation) they are generally found to be consistent (e.g., Beck 2000; Vallée 1995). In addition, the crucial assumption of the minimum energy argument, namely that the energy density in the magnetic field is roughly equal to the energy density in cosmic rays, is confirmed locally in the Galaxy using γ -ray observations (Strong et al. 2000).

In keeping with previous studies, our results in Figure 1 show that in normal star-forming galaxies, $B_{\text{min}} \sim B_{\text{eq}}$. However, the striking result from Figure 1 is that the starburst galaxies systematically have $B_{\text{min}} < B_{\text{eq}}$. The ratio $\eta_{\text{min}} = (B_{\text{min}}^2/8\pi)/P$ is a strongly decreasing function of Σ_g ; for a typical starburst such as M82, $\eta_{\text{min}} \sim 10^{-2}$, while for Arp 220, $\eta_{\text{min}} \sim 10^{-4}$.⁹

If the minimum energy magnetic field strength estimate is applicable, the direct implication of Figure 1 is that in starbursts, magnetic fields are dynamically weak compared to gravity in the phase of the ISM in which the radio emitting electrons reside. Because of the potential importance of this conclusion, it is worth critically examining the applicability of the minimum energy estimate in the context of luminous starbursts (see Beck & Krause 2005 for a more general discussion). The minimum energy argument rests on the assumption that the magnetic energy density is comparable to the cosmic ray energy density. Given that the magnetic field and cosmic rays could have rather different energy generation and dissipation mechanisms (‘‘sources and sinks’’), the generic applicability of this assumption is unclear.

In the context of local spirals, one argument in favor of the minimum energy estimate is precisely that it implies a total cosmic ray + magnetic energy density in approximate equipartition with gravity. If $B \neq B_{\text{min}}$, the net cosmic ray + magnetic energy density would exceed the gravitational binding energy of the gas, and the field and relativistic particles would presumably escape from the galactic disk (e.g., Parker 1965, 1966; Duric 1990). This provides a natural mechanism by which the magnetic field strength can adjust to a value of $\sim B_{\text{min}}$. However, such an argument does not apply in starbursts given that the minimum energy argument itself implies $\eta_{\text{min}} \ll 1$ (Fig. 1).

A more significant worry concerning the applicability of the minimum energy argument in starbursts is that strong syn-

⁹ Free-free absorption may suppress the observed radio flux density at GHz frequencies in dense starbursts (e.g., Condon et al. 1991). However, even in our most extreme case, the ULIRG Arp 220, this correction amounts to a small increase ($\sim 10\%$) in our inferred B_{min} . Another uncertainty is the contribution of free-free emission to the observed radio flux. At GHz frequencies the thermal fraction is of order 10% for normal star-forming galaxies (e.g., Niklas 1995). For starbursts the thermal fraction is less certain. In any case, subtracting the thermal contribution to the radio luminosity would decrease the inferred B_{min} , strengthening our conclusion that $B_{\text{min}} \ll B_{\text{eq}}$ in starbursts.

chrotron and inverse Compton (IC) losses could lead to rapid electron cooling. If the steady state electron energy density is significantly lower as a result, then the minimum energy magnetic field is an *underestimate*.

In the following sections we critically review independent observational and theoretical constraints on the magnetic fields in starbursts. We begin by summarizing arguments in favor of $B \sim B_{\min}$ and against the hypothesis that magnetic fields in starbursts are significantly larger. Several of these arguments draw heavily on existing results in the literature, but are worth reviewing in the present context. Rebuttals to these arguments are given in §4, where we also provide independent arguments in favor of $B \gg B_{\min}$.

3. ARGUMENTS FOR $B \sim B_{\min}$ IN STARBURST GALAXIES

3.1. Zeeman Measurements

To our knowledge, there are no extragalactic detections of Zeeman splitting. In four ULIRGs, however, Killeen et al. (1996) derive upper limits of $B \lesssim 3-5$ mG using OH masers. These limits are larger than the minimum energy estimate of ~ 1 mG for ULIRGs, but are a factor of ~ 5 smaller than B_{eq} for Arp 220 in Figure 1. In our own Galaxy OH masers trace regions of higher than average surface density and magnetic field strength, with $B \approx 2-10$ mG (e.g., Fish et al. 2003); it is unlikely that the opposite is true in ULIRGs, in which case the Killeen et al. (1996) upper limits argue against $B \sim B_{\text{eq}}$. However, a larger sample of Zeeman measurements is needed, particularly for galaxies which also have reliable gas surface density measurements.

3.2. Cooling Breaks

The synchrotron cooling timescale for cosmic ray electrons emitting at frequency ν is

$$\tau_{\text{syn}} \approx 10^6 B_{100}^{-3/2} \nu_{\text{GHz}}^{-1/2} \text{ yr}, \quad (4)$$

where $B_{100} = B/100 \mu\text{G}$. IC losses can be appreciable as well and lead to cooling on a timescale

$$\tau_{\text{IC}} \approx 5 \times 10^5 B_{100}^{1/2} \nu_{\text{GHz}}^{-1/2} U_{\text{ph},-9}^{-1} \text{ yr}, \quad (5)$$

where $U_{\text{ph}} = 10^{-9} U_{\text{ph},-9}$ ergs cm^{-3} is the energy density of (primarily infrared) photons in the starburst.

The cooling timescale for electrons can be indirectly constrained using the radio spectrum. For continuous injection of relativistic electrons, if the cooling time

$$\tau_{\text{cool}}^{-1} = \tau_{\text{syn}}^{-1} + \tau_{\text{IC}}^{-1} \quad (6)$$

of the electrons emitting at frequency ν is shorter than the escape time from the galactic disk, the radio spectrum will steepen by $\Delta\alpha = 1/2$ at higher frequencies, where $F_\nu \propto \nu^{-\alpha}$. For canonical electron power-law indices of $p = 2$ expected theoretically for strong shocks (e.g., Blandford & Eichler 1987) and observed *in situ* in some supernova remnants (e.g., Aharonian et al. 2005; Brogan et al. 2005), $\alpha = 1/2$ in the absence of cooling and steepens to $\alpha = 1$ in the presence of cooling. The escape time of relativistic particles from the galactic disk is uncertain. In local spirals the escape is due to diffusion across the magnetic field, while in starbursts it may be much more rapid due to advection out of the galaxy with a galactic wind. The escape time in the latter case is roughly

$$\tau_{\text{esc}} \sim h/v_w \sim 3 \times 10^5 h_{100} v_{500}^{-1} \text{ yr}, \quad (7)$$

where $h = 100 h_{100}$ pc is the scale height of the galactic disk and $v_w = 500 v_{500}$ km s^{-1} is the speed of the galactic wind (see, e.g., Martin 1999 for estimates of the latter).

The radio spectra of both normal spirals and luminous starbursts are similar with $\langle\alpha\rangle \approx 0.75$ from $\approx 1-10$ GHz (e.g., Condon et al. 1991; Condon 1992; Niklas et al. 1997). There appears to be no strong variation of α with the luminosity of the galaxy (though Niklas et al. 1997 note a weak trend for starbursts to have somewhat flatter nonthermal spectral indices). The lack of a systematic variation of the spectral index with luminosity, together with the fact that the observed radio spectra are significantly flatter than expected for a ‘‘cooled’’ electron distribution, suggests that $\tau_{\text{cool}} \gtrsim \tau_{\text{esc}}$, even in luminous starbursts. Using equation (7) to estimate τ_{esc} , equation (4) then implies field strengths $\lesssim 2 \times 10^{-4}$ G, reasonably consistent with the minimum energy estimates for the starbursts in Figure 1 and inconsistent with $B \gg B_{\min}$.

3.3. Synchrotron Halos

The spatial variation of the radio spectrum can provide a more stringent constraint on the importance of electron cooling than the integrated radio spectrum alone. To take a concrete example, observations of M82 by Klein et al. (1988) and Seaquist & Odegard (1991) reveal an extended radio halo along the minor axis of M82, coincident with the observed galactic wind. The radio spectrum at GHz frequencies is observed to be roughly constant in the disk of M82, but to steepen significantly in the halo a distance $h_{\text{break}} \sim 300$ pc above the midplane. The usual interpretation of this halo is that relativistic electrons generated in the starburst are advected out with the galactic wind. The steepening at $h_{\text{break}} \sim 300$ pc can then be modeled as a consequence of electron cooling (e.g., Seaquist & Odegard 1991). The radio emitting electrons in the halo must thus have $h_{\text{break}} \sim \tau_{\text{cool}} v_w$. This approximate equality can be used to put a limit on the magnetic field in the disk of M82. For example, the equipartition field of $B_{\text{eq}} \approx 1.6$ mG in M82 (see Fig. 1) implies a synchrotron cooling time of $\tau_{\text{syn}} \sim 10^4$ yrs, which, in turn, requires an unphysically large $v_w \sim 30,000$ km s^{-1} to explain the observed scale of the spectral break in M82. Thus a magnetic field strength of $\sim B_{\text{eq}}$ is strongly disfavored under the interpretation that the synchrotron halo in M82 is due to electrons accelerated in the disk and advected out in a galactic wind. By contrast, a field strength of $B \sim B_{\min}$ implies $v_w \sim 500$ km s^{-1} to explain a spectral break at $h_{\text{break}} \sim 300$ pc — much more reasonable in the context of galactic winds. Thus, the spatial variation of the radio spectrum in M82 appears to provide independent evidence that $\tau_{\text{cool}} \gtrsim \tau_{\text{esc}}$ in the galactic disk and hence that $B \sim B_{\min} \ll B_{\text{eq}}$.

In fact, more careful estimates account for both IC cooling and adiabatic cooling of relativistic electrons as they are advected out into the halo. This increases the required wind speed by a factor of few to ~ 2000 km s^{-1} (e.g., Seaquist & Odegard 1991). Although this is substantially smaller than the speed of $\sim 30,000$ km s^{-1} required for $B \sim B_{\text{eq}}$, it is larger than the inferred speeds of galactic winds (e.g., Martin 1999) and is comparable to the initial velocity of supernova ejecta. One cannot, however, rule out a very low density phase of a galactic wind with the required velocity ~ 2000 km s^{-1} .

We note that NGC 253 (Carilli et al. 1992), NGC 1569 (Israel & de Bruyn 1988; Lisenfeld et al. 2004), NGC 4631 (Ekers & Sancisi 1977), NGC 891 (Allen, Sancisi, & Baldwin

1978), and NGC 4666 (Dahlem et al. 1997) all exhibit radio halos qualitatively similar to those in M82. Unfortunately, with the exception of NGC 253, these systems have lower gas surface densities than M82 and lie in the part of Figure 1 where $B_{\min} \sim B_{\text{eq}}$. Clearly, a more extensive survey for low surface brightness extended radio emission around starbursts with $\Sigma_g \sim 1 \text{ g cm}^{-2}$ would be very useful in discriminating between the minimum energy and equipartition magnetic field strengths (see Table 2).

4. ARGUMENTS FOR $B \gg B_{\min}$ IN STARBURST GALAXIES

In this section we rebut the arguments for $B \sim B_{\min}$ presented in Sections 3.2 and 3.3 and provide additional evidence that $B \gg B_{\min}$. Most of this section centers on showing that $\tau_{\text{cool}} \lesssim \tau_{\text{esc}}$ is consistent with radio observations of starbursts.

4.1. Understanding B_{\min} as a Function of Σ_g

A magnetic field strength of $B \gg B_{\min}$ in starbursts would imply that the cooling time for relativistic electrons is very short compared to the escape time ($\tau_{\text{cool}} \ll \tau_{\text{esc}}$). To show this, we assume that $B = \eta^{1/2} B_{\text{eq}}$, that $\tau_{\text{esc}} = 10^6 \tau_{\text{esc},6} \text{ yr}$, and we combine equations (3) and (4) to estimate that

$$\frac{\tau_{\text{syn}}}{\tau_{\text{esc}}} \sim 0.01 \Sigma_g^{-3/2} \eta^{-3/4} \nu_{\text{GHz}}^{-1/2} \tau_{\text{esc},6}^{-1}. \quad (8)$$

For $\Sigma_g \gtrsim 0.05 \tau_{\text{esc},6}^{-2/3} \eta^{-1/2} \text{ g cm}^{-2}$, equation (8) implies that $\tau_{\text{syn}} < \tau_{\text{esc}}$ for electrons emitting at GHz frequencies. Including IC cooling decreases this critical surface density by a factor of order unity. In addition, for lower surface density galaxies, the electron escape time becomes increasingly determined by diffusion across the magnetic field rather than escape in a galactic wind. This likely increases τ_{esc} substantially and thus decreases the critical surface density where $\tau_{\text{syn}} \sim \tau_{\text{esc}}$.

The above considerations show that if $B \gg B_{\min}$ then nearly all of the starbursts in Figure 1 are in the limit where $\tau_{\text{cool}} < \tau_{\text{esc}}$. Our observationally inferred results for $B_{\min}(\Sigma_g)$ can be understood quantitatively in this limit as follows. In the rapidly cooling limit, the electrons radiate all of the energy supplied to them by supernova shocks and thus the radio flux per unit volume is determined by the supernova rate per unit volume:

$$\nu L_\nu / V \propto \dot{\Sigma}_* / h, \quad (9)$$

where $\dot{\Sigma}_*$ is the star formation rate per unit area and V is the radio emitting volume. Using the Schmidt Law for star formation ($\dot{\Sigma}_* \propto \Sigma_g^{7/5}$; Kennicutt 1998) and equation (1), we find

$$B_{\min} \propto \Sigma_g^{2/5} h^{-2/7}. \quad (10)$$

To estimate the proportionality constant in equation (10), we assume that $10^{-3} \xi$ of each SN's energy is supplied to relativistic electrons (and is radiated away), in which case equation (10) becomes

$$B_{\min} \approx 7 \times 10^{-5} \delta_2^{2/7} \xi^{2/7} \Sigma_g^{2/5} h_{100}^{-2/7} \nu_{\text{GHz}}^{-1/7} \text{ G}, \quad (11)$$

Taking $h \sim \text{constant}$ and $\xi = 10$ (see §4.2), we plot equation (11) in Figure 1 (dashed line) and find that it is in reasonable agreement with the results for starbursts. This provides strong support for the hypothesis that $\tau_{\text{cool}} \lesssim \tau_{\text{esc}}$ in these systems. Furthermore, the agreement between the starburst data and equation (11) emphasizes that the inferred minimum energy field in starbursts is not a reliable magnetic field measurement, but rather simply reflects the fact that the radio flux is proportional to the star formation rate (eq. [9]).

4.2. The FIR-Radio Correlation

Equation (9) implies a linear correlation between the FIR luminosity (L_{FIR}) and the radio luminosity (L_{rad}) of galaxies. Such a correlation is in fact observed over more than four orders of magnitude in L_{FIR} (van der Kruit 1971, 1973; Helou et al. 1985; Condon 1992; Yun, Reddy, & Condon 2001). Equation (9) is a consequence of the fact that if $\tau_{\text{cool}} \lesssim \tau_{\text{esc}}$, then the radio flux is essentially independent of the magnetic field strength and depends only on the rate at which energy is supplied to the relativistic electrons. The linearity of the FIR-radio correlation then follows naturally from the fact that the supernova rate is proportional to the star formation rate (e.g., the ‘‘calorimeter’’ theory; Völk 1989; see also Bressan et al. 2002). Thus as long as $\tau_{\text{cool}} \lesssim \tau_{\text{esc}}$ one can account for the observed linear FIR-radio correlation with no fine tuning.

By contrast, if $\tau_{\text{cool}} \gtrsim \tau_{\text{esc}}$ (as argued in §3.2 & 3.3) then significant fine tuning is required to explain the FIR-radio correlation. Because the synchrotron cooling timescale (eq. [4]) varies by a factor of $\sim 10^3$ for the systems in Figure 1 (a factor of ~ 60 for the starbursts alone), the escape timescale would have to vary by exactly the same factor in order to preserve a linear FIR-radio correlation. We believe that this level of fine tuning argues strongly against $\tau_{\text{cool}} \gtrsim \tau_{\text{esc}}$ (and thus indirectly against $B \sim B_{\min}$).

The magnitude of the radio flux from star-forming galaxies is also fully consistent with the hypothesis that $\tau_{\text{cool}} \lesssim \tau_{\text{esc}}$. To demonstrate this, we note that if each supernova supplies an energy of $\xi 10^{48}$ ergs to cosmic ray electrons with a spectral index $p = 2$, and if $\tau_{\text{cool}} \ll \tau_{\text{esc}}$, then the radio luminosity should be related to the FIR luminosity via $\nu L_\nu \approx 10^{-5} \xi L_{\text{IR}} / 2 \ln(\gamma_{\text{max}}) \approx 2.5 \times 10^{-7} \xi L_{\text{IR}}$, where γ_{max} is the maximum Lorentz factor of the accelerated electrons. For comparison, the 1.4 GHz FIR-radio correlation from Yun et al. (2001) is $\nu L_\nu \approx 2 \times 10^{-6} L_{\text{IR}}$. This implies that $\xi \approx 8$ is needed to account for the FIR-radio correlation. That is, $\approx 0.8\%$ of each supernova's energy is radiated away as synchrotron radiation. This is similar to standard estimates for the fraction of SN energy *supplied* to relativistic electrons (see, e.g., §2.2.2 of Keshet et al. 2003 for a summary), which supports the hypothesis that $\tau_{\text{cool}} \lesssim \tau_{\text{esc}}$. In particular, this argument rules out the possibility that $\tau_{\text{cool}} \gg \tau_{\text{esc}}$, since in this case the amount of supernova energy supplied to cosmic rays would have to be prohibitively large ($\xi \gg 1$).

An oft-cited objection to the calorimeter model for the FIR-radio correlation is that the nonthermal radio spectra of galaxies should then be significantly steeper than are observed because of strong synchrotron cooling (see §3.2; e.g., Condon 1992). In §4.3 we show that ionization and bremsstrahlung losses can systematically flatten the radio spectra of starbursts even when $\tau_{\text{cool}} \ll \tau_{\text{esc}}$, providing much better agreement with observations.

Equation (8) implies that $\tau_{\text{syn}} \gtrsim \tau_{\text{esc}}$ for $\Sigma_g \lesssim 0.005 (0.05) \text{ g cm}^{-2}$, if $\tau_{\text{esc}} \approx 3 \times 10^7 (10^6) \text{ yr}$. The former value of τ_{esc} is comparable to that estimated for the Milky Way (Garcia-Munoz et al. 1977; Connell 1998). According to the arguments presented in this section, the calorimeter theory for the FIR-radio correlation thus does not apply to low surface density normal star-forming galaxies. One might then expect a change in the FIR-radio correlation at low Σ_g because a smaller fraction of the electron energy is radiated away. Observationally, there is only a very mild suppression in the ratio

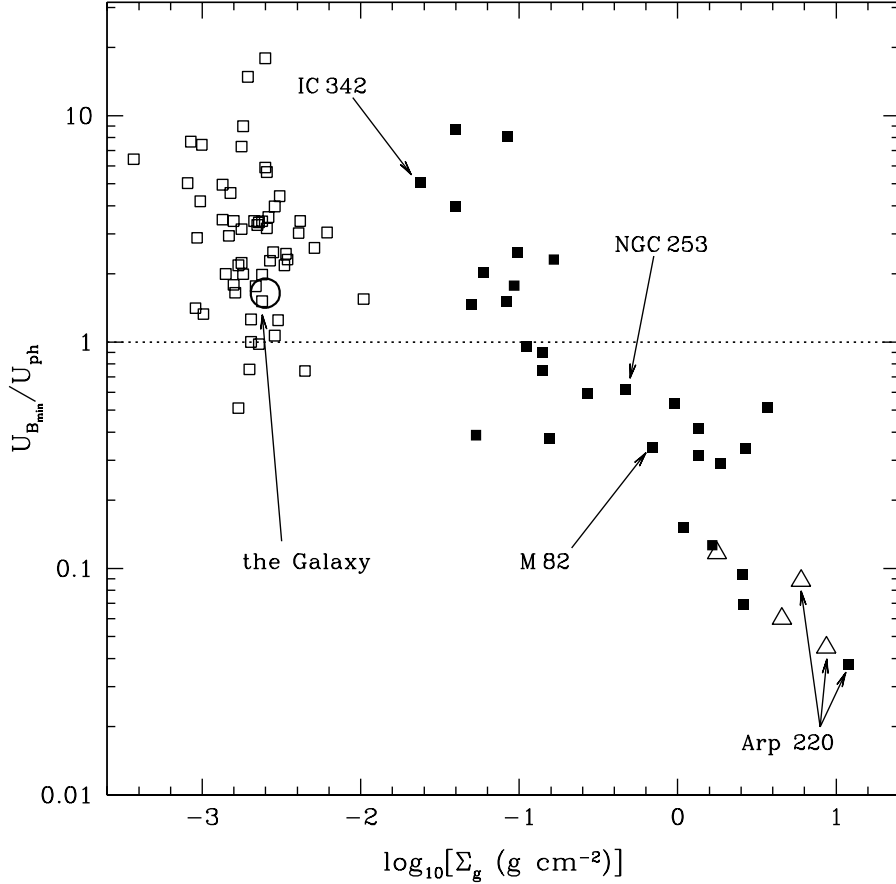


FIG. 2.— The ratio of the minimum energy magnetic energy density to the photon energy density ($U_{B_{\min}}/U_{ph}$) as a function of the gas surface density (Σ_g). The symbols are the same as those in Fig. 1. U_{ph} is calculated using eq. (12) (see also eq. [13]) for all systems except the Galaxy, for which we take $F = L/\pi R^2$ with $L = 1.5 \times 10^{10} L_{\odot}$ and $R = 8.5$ kpc (as appropriate for the estimate of B_{\min} at the solar circle). $U_B < U_{ph}$ is difficult to reconcile with the linearity of the FIR-radio correlation and suggests that the minimum energy field strength is an underestimate for luminous starbursts.

of the radio to FIR luminosities for low-luminosity galaxies (Yun et al. 2001). Bell (2003) has shown, however, that this is in part because neither the radio nor the FIR emission from low luminosity galaxies are good proxies for the total star formation rate. Because the focus of this paper is on starburst galaxies, we defer a more detailed analysis of the connection between the FIR-radio correlation in normal spirals and starbursts to a future paper.

4.2.1. Synchrotron versus Inverse Compton Cooling

Regardless of the value of $\tau_{\text{cool}}/\tau_{\text{esc}}$, the linearity of the FIR-radio correlation suggests that the synchrotron cooling timescale τ_{syn} (eq. [4]) must be shorter than the IC cooling timescale τ_{IC} (eq. [5]). This in turn implies that $U_B \gtrsim U_{ph}$. If this constraint is not satisfied, any variation in U_B/U_{ph} would imply large changes in the fraction of cosmic ray electron energy radiated via synchrotron radiation. A linear FIR-radio correlation would then require significant fine tuning.

In Figure 2 we plot the ratio $(B_{\min}^2/8\pi)/U_{ph}$ versus gas surface density for the sample of galaxies from Figure 1 (Tables 1- 3). The photon energy density is computed using

$$U_{ph} = \frac{F}{c} = \epsilon \dot{\Sigma}_{\star} c, \quad (12)$$

where F is the radiative flux, $\dot{\Sigma}_{\star}$ is the star formation rate per unit area, and we take $\epsilon = 3.8 \times 10^{-4}$ for consistency with Kennicutt (1998). Above the dotted line in Figure 2, $U_{B_{\min}}/U_{ph} > 1$, $\tau_{\text{syn}} < \tau_{\text{IC}}$, and synchrotron dominates IC as the primary coolant for the relativistic electrons. Below the dotted line $\tau_{\text{syn}} > \tau_{\text{IC}}$ and IC dominates.

Figure 2 shows that for high surface density starbursts the minimum energy argument implies magnetic energy densities smaller than the photon energy density. For the most extreme case of Arp 220 (and ULIRGs in general), the minimum energy estimate implies $U_B/U_{ph} \sim 0.1$. For most starbursts in Figure 2, a modest increase of B by a factor of $\sim 2-3$ would lead to $U_B \gtrsim U_{ph}$. This is plausibly within the uncertainties of the minimum energy estimate — and is a rather minor correction on the scale of B_{eq}/B_{\min} in Figure 1 — but does suggest that B_{\min} is an underestimate.

Equation (12) may significantly underestimate U_{ph} for galaxies with $\Sigma_g \gtrsim 0.5 \text{ g cm}^{-2}$ because the ISM is optically thick to its own FIR radiation in these systems. In this case,

$$U_{ph} = \frac{\tau_{\text{IR}} F}{c} \approx \tau_{\text{IR}} \epsilon \dot{\Sigma}_{\star} c, \quad (13)$$

where $\tau_{\text{IR}} \approx \kappa_{\text{IR}} \Sigma_g$ is the optical depth of the galactic disk to

the IR radiation and $\kappa_{IR} \approx 3 - 10 \text{ cm}^2 \text{ g}^{-1}$ is the temperature-dependent dust opacity in the FIR (Thompson, Quataert, & Murray 2005). In principle, this factor of τ_{IR} could increase U_{ph} by a factor of 10–100 for ULIRGs. If one requires that $U_B > U_{ph}$ in order to satisfy the FIR-radio correlation, the necessary field strength would then be $\gg B_{\min}$, and perhaps as large as $\sim B_{\text{eq}}$. The applicability of equation (13) hinges, however, on the assumption that the radio emitting electrons are co-spatial with optically thick gas at the average density of the ISM. If the radio emitting electrons are in a lower-than-average density (optically thin) environment, then equation (12) is still valid.

4.3. Cooling Breaks

In §3.2 we noted that because starburst radio spectra do not show significant evidence for synchrotron cooling, the straightforward interpretation is that $\tau_{\text{cool}} \gtrsim \tau_{\text{esc}}$ and, hence, $B \sim B_{\min}$. One difficulty with this conclusion is provided by ULIRGs such as Arp 220, where the IC cooling time alone is $\sim 10^4$ yrs. Unless $h \lesssim 10$ pc, the cooling time in ULIRGs is shorter than the advection time across the galactic disk, for reasonable values of the advection velocity. Given that the size of the radio emitting region resolved by the VLA in ULIRGs is typically ~ 100 pc (Condon et al. 1991), one might thus expect the nonthermal spectrum to be systematically steeper in ULIRGs than in other starbursts.¹⁰ This does not however, appear to be the case (Condon et al. 1991; see also Fig. 19 of Downes & Solomon 1998 for the case of Arp 220). The lack of a systematic difference between the radio spectral indices of ULIRGs and other systems raises significant questions about the extent to which the radio spectra can be easily used to constrain the electron cooling time and thus the magnetic field strength.

We suggest that the radio spectra of starbursts are in fact compatible with $\tau_{\text{cool}} \ll \tau_{\text{esc}}$ because of the effect of ionization and bremsstrahlung losses on the low energy part of the electron distribution function. The timescale for a relativistic electron that emits synchrotron radiation at frequency ν to lose its energy ionizing neutral hydrogen of density $n = 10 n_{10} \text{ cm}^{-3}$ is

$$\tau_{\text{ion}} \approx 10^7 n_{10}^{-1} \nu_{\text{GHz}}^{1/2} B_{100}^{-1/2} \text{ yr.} \quad (14)$$

Relativistic electrons also lose energy to bremsstrahlung emission on ambient neutral nuclei, on a timescale

$$\tau_{\text{brem}} \approx 3 \times 10^6 n_{10}^{-1} \text{ yr.} \quad (15)$$

Setting $B = \eta^{1/2} B_{\text{eq}}$ and $n = f \langle n \rangle = f \Sigma_g / 2 h m_p$ we find that the ratio of the ionization loss time to the synchrotron cooling time is

$$\frac{\tau_{\text{ion}}}{\tau_{\text{syn}}} \approx 1.6 \nu_{\text{GHz}} h_{100} f^{-1} \eta^{1/2} \quad (16)$$

and that the ratio of the bremsstrahlung loss time to the synchrotron cooling time is

$$\frac{\tau_{\text{brem}}}{\tau_{\text{syn}}} \approx 2.4 \nu_{\text{GHz}}^{1/2} h_{100} f^{-1} \eta^{3/4} \Sigma_g^{1/2}, \quad (17)$$

where $h_{100} = h/100$ pc is the gas scale height. Equations (16) & (17) show that if the cosmic ray electrons interact with

¹⁰ Although the radio sizes are ~ 100 pc, a small scale height for ULIRGs is not ruled out: for a random velocity δv , the scale height of a galactic disk is $h \approx \delta v^2 / 2\pi G \Sigma$, which implies $h \approx 10$ pc for the observed values of $\delta v \approx 100 \text{ km s}^{-1}$ and $\Sigma \approx 10 \text{ g cm}^{-2}$ in Arp 220 (e.g., Scoville et al. 1997).

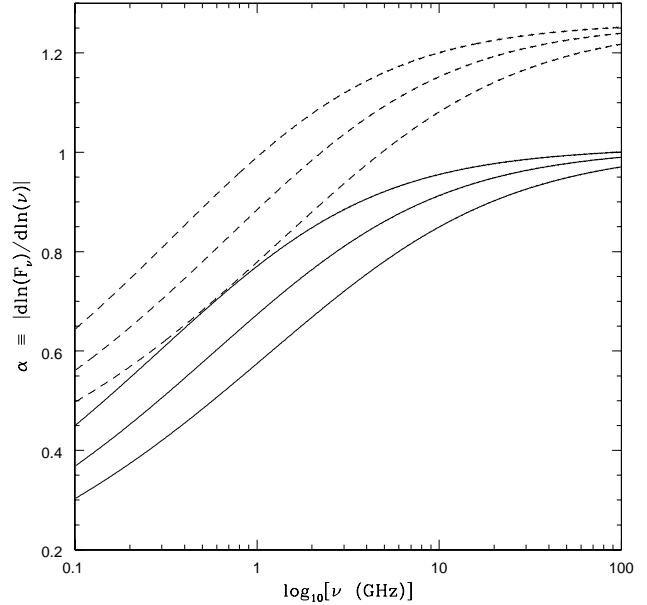


FIG. 3.— Predicted radio spectral index as a function of frequency. Electrons are injected with $n(\gamma) \propto \gamma^{-p}$, with $p=2$ (solid lines) and $p=2.5$ (dashed lines), and lose energy through synchrotron radiation, bremsstrahlung, and ionization losses. Escape is neglected, which corresponds to the limit $\tau_{\text{cool}} \ll \tau_{\text{esc}}$. The calculations assume $\Sigma_g = 1 \text{ g cm}^{-2}$, $\eta = 1$, $h_{100} = 1$, and $f = 1, 0.5, 0.25$ (from bottom to top). Ionization losses flatten the radio spectrum at low frequencies. Therefore, even in the limit $\tau_{\text{cool}} \ll \tau_{\text{esc}}$, spectral indices at GHz frequencies are less than the canonical value of $\alpha = 1$ (for $p=2$) appropriate for strong synchrotron cooling. This provides much better agreement with the observed radio spectra of starbursts.

gas at the mean density of the ISM ($f \sim 1$) ionization and bremsstrahlung losses can significantly modify the distribution function for electrons emitting at \sim GHz frequencies.

Under the action of ionization losses alone, low energy cosmic rays lose energy more rapidly than high energy cosmic rays (the bremsstrahlung loss time is independent of electron energy). The opposite is true for synchrotron losses. For this reason, ionization losses can systematically decrease the spectral index from what one would expect for a synchrotron-cooled electron distribution ($\alpha \approx 1 - 1.25$). To demonstrate this explicitly, we have calculated the steady state electron distribution function for a model in which relativistic electrons are injected with a spectral index p and lose energy via synchrotron radiation, bremsstrahlung losses, and ionization losses. Escape is neglected, which corresponds to the limit $\tau_{\text{cool}} \ll \tau_{\text{esc}}$. Figure 3 shows the resulting synchrotron spectral slope α as a function of frequency. The solid lines are for $p=2$ and the dashed lines are for $p=2.5$. The calculations shown in Figure 3 assume $\Sigma_g = 1 \text{ g cm}^{-2}$, $\eta = 1$, $h_{100} = 1$, and $f = 1, 0.5$, and 0.25 (from bottom to top).

The spectral indices in Figure 3 at GHz frequencies are compatible with the observed values even in the presence of strong cooling. We find similar results for reasonable variations of our model parameters. For example, if $p=2$, $\eta = 0.1$, and $f = 0.25$, we find $\alpha \approx 0.6$ at 1 GHz from $\Sigma_g \approx 0.1 - 10 \text{ g cm}^{-2}$ and $\alpha \approx 0.7 - 0.8$ at 5 GHz over the same range of Σ_g . Our calculations predict that the non-thermal spectral index should steepen to $\alpha \sim 1$ at sufficiently high frequencies, but this may be difficult to detect because of free-free

emission. A second prediction of this model is that the radio spectral index should be larger at high frequencies than it is at low frequencies, with a transition at \sim GHz frequencies where the ionization, bremsstrahlung, and synchrotron loss times are comparable (see eqns. [16] & [17]). For example, in the model from Figure 3 with $p = 2$ and $f = 0.5$ (the middle solid line), the effective spectral index from 1–10 GHz is $\alpha = 0.8$, whereas from 0.1–1 GHz it is $\alpha = 0.55$. Using the radio data in Table 2, as well as 57.5, 151, 408, 750, and 4850 MHz data available in the NASA Extragalactic Database (from Hales et al. 1993; Ficarra et al. 1985; Israel & Mahoney 1990; Becker et al. 1991; McCutcheon 1973; Waldram et al. 1996; Heeschen & Wade 1964; Large et al. 1981; Griffith et al. 1995; Kuehr et al. 1981), and additional data from Oly & Israel (1993) (for NGC 3504), Irwin & Saikia (2003) (for NGC 3079), and Hummel et al. (1991) (for NGC 891), we find that for the sample of starburst galaxies considered in this paper the spectral index below 1 GHz is indeed typically flatter than that above 1 GHz by $\Delta\alpha \approx 0.3$ (although there are some exceptions and scatter).

Although encouraging, a larger and more homogeneous sample of data is clearly needed to test our predictions of spectral index variations as a function of frequency. In addition, low frequency radio emission may be strongly modified by free-free absorption in many starbursts. Moreover, electrons emitting at \sim 100 MHz in a \sim mG field have energies of \sim 100 MeV. At these energies secondary electrons produced by charged pion decay are important and may significantly modify the electron spectrum as well.

Because the synchrotron, ionization, and bremsstrahlung loss rates all scale differently with the gas density and magnetic field strength, there is no guarantee that the linearity of the FIR-radio correlation is preserved under the influence of ionization and bremsstrahlung losses. To assess this, Figure 4 shows model calculations of $L_{\text{FIR}}/L_{\text{rad}}$ as a function of Σ_g . The synchrotron flux at 1 GHz is calculated assuming that electrons are injected with a $p = 2$ spectrum, and lose energy via synchrotron, ionization, and bremsstrahlung losses (as before, escape is neglected). The FIR luminosity is assumed to be proportional to the rate at which energy is supplied to relativistic electrons. The models shown in Figure 4 assume that $f = 0.5$ ($n = 0.5\langle n \rangle$), $h_{100} = 1$, and that $B \propto \Sigma_g^a$ with $a = 1, 0.9, 0.8$, and 0.7 (bottom to top; see Fig. 1 for the $B(\Sigma_g)$ curves). All of the assumed models for $B(\Sigma_g)$ have $B \gg B_{\text{min}}$ for luminous starbursts.

Figure 4 demonstrates that the predicted FIR-radio correlation is linear to better than a factor of 2 over 3 orders of magnitude in Σ_g . The models with $a = 0.7, 0.8$, and 0.9 provide particularly good agreement with the observed linearity of the FIR-radio correlation. Because galaxies of a given Σ_g can have a range of FIR luminosities (depending on galaxy size), the systematic trends in Figure 4 may show up in part as scatter in the canonical plots of $L_{\text{FIR}}/L_{\text{rad}}$ vs. L_{FIR} ; the \lesssim factor of 2 variation in Figure 4 is consistent with the observed scatter in the FIR-radio correlation. The approximate constancy of $L_{\text{FIR}}/L_{\text{rad}}$ in Figure 4 arises because if $f \sim 1$ and $B \gg B_{\text{min}}$, then $\tau_{\text{syn}}/(\tau_{\text{ion}}^{-1} + \tau_{\text{brem}}^{-1})^{-1}$ is relatively constant over most of the parameter space relevant to observed starbursts.

In §4.2 we estimated that $\approx 0.8\%$ of the energy of each supernova must be supplied to relativistic electrons to account for the magnitude of the ≈ 1.4 GHz radio flux from starburst galaxies, taking into account synchrotron radiation alone and

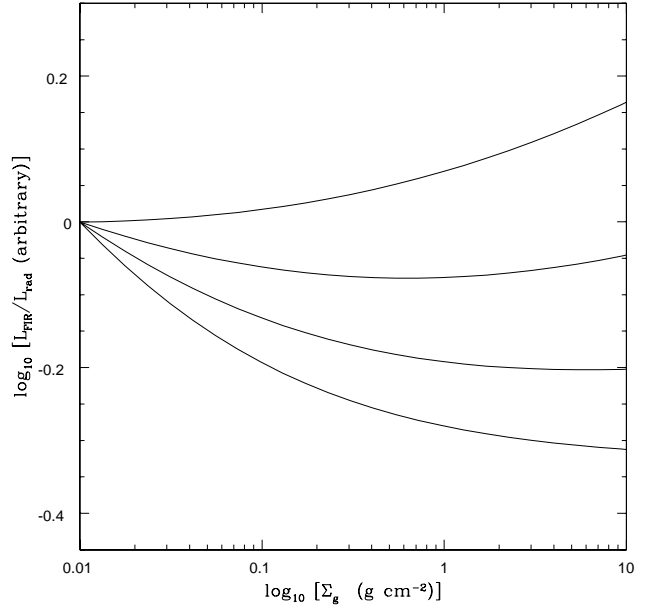


FIG. 4.— Predicted ratio of the FIR to 1 GHz synchrotron luminosity as a function of gas surface density Σ_g . Electrons are injected with a $p = 2$ spectrum and lose energy through synchrotron radiation and ionization and bremsstrahlung losses; escape is neglected. The FIR luminosity is assumed to be proportional to the total rate at which energy is supplied to relativistic electrons. The calculations assume that $f = 0.5$ ($n = 0.5\langle n \rangle$) and that $B \propto \Sigma_g^a$ with $a = 1, 0.9, 0.8$, and 0.7 (bottom to top) and $B = B_{\text{eq}}$ at $\Sigma_g = 0.01 \text{ g cm}^{-2}$ (see Fig. 1 for these scalings). These results demonstrate that although ionization and bremsstrahlung losses modify the radio spectra of starbursts (Fig. 3), they nonetheless maintain a nearly linear FIR-radio correlation, in agreement with observations.

assuming electrons are injected with a $p = 2$ spectrum. If ionization and bremsstrahlung losses are important in starbursts, as argued in this section, then the required energy injection rate increases to $\approx 1.6\%$ of the supernova energy. In addition, if the electron injection spectrum is $p = 2.2$, then the required energy injection increases by an additional factor ≈ 2 .

In contrast to the results of Figure 4, in a model in which $f = 0.5$ and $B \propto \Sigma_g^{0.4}$, which corresponds to the observed scaling of $B_{\text{min}}(\Sigma_g)$ in Figure 1, the ratio of the FIR to radio luminosities increases by a factor of ≈ 10 from $\Sigma_g = 0.01 \text{ g cm}^{-2}$ to $\Sigma_g = 10 \text{ g cm}^{-2}$ because of the increasing suppression of the radio flux by bremsstrahlung losses. Thus field strengths $\approx B_{\text{min}}$ are only consistent with the observed radio emission from starbursts if cosmic-ray electrons interact with gas at much less than the mean density of the ISM ($f \ll 1$).

To summarize this subsection, if $B \gg B_{\text{min}}$ and if cosmic-ray electrons interact with gas at approximately the mean density of the ISM, ionization and bremsstrahlung losses will systematically flatten the nonthermal spectra of starburst galaxies (Fig. 3) and yet maintain the linearity of the FIR-radio correlation (Fig. 4). This eliminates one of the strongest arguments against $\tau_{\text{cool}} \ll \tau_{\text{esc}}$ and argues for $B \gg B_{\text{min}}$ in starbursts.

4.4. Pion Production

An independent test of the density of the ISM in which the cosmic rays reside can be provided by gamma-ray emission from neutral pion decay. The timescale for cosmic ray

protons to lose their energy to pion production is $t_{\text{pion}} \sim 10^8 (n/1 \text{ cm}^{-3})^{-1} \text{ yr}$. If $n \sim \langle n \rangle$, this is significantly shorter than τ_{esc} in starbursts (see eq. [7]) and so pion production will lead to a substantial γ -ray luminosity. Assuming that 10% of the energy of each supernova is supplied to relativistic protons with a spectral index $p = 2$, and that $\approx 1/3$ of this energy goes into γ -rays rather than neutrinos or pairs, we estimate a γ -ray luminosity from neutral pion decay in starbursts of $\nu L_\nu \approx 3 \times 10^{-4} L_{\text{IR}} / \ln(\gamma_{\text{max}}) \approx 2 \times 10^{-5} L_{\text{IR}}$, where γ_{max} is the maximum Lorentz factor of the accelerated protons and the estimate is only applicable above $\approx 100 \text{ MeV}$ (see Torres 2004 for more detailed calculations). This predicted flux is just below the EGRET upper limits for systems such as M82 and Arp 220 (Cillis et al. 2005), but should be detectable with *GLAST*. Because the timescales for electron ionization and bremsstrahlung losses and proton pion losses are quite similar, detection of gamma-ray emission at this level would also confirm the importance of ionization and bremsstrahlung losses for the observed radio spectra of starbursts.

Relativistic protons lose $\approx 2/3$ of their energy to the production of charged pions, which subsequently decay into high energy neutrinos and electron/positron pairs; the pairs receive $\approx 1/4$ of the pion energy. Thus if $\sim 10\%$ of the energy of each supernova is supplied to relativistic protons, and if $t_{\text{pion}} \ll t_{\text{esc}}$, then $\sim 1.5\%$ of the energy of each supernova goes into secondary electrons and positrons. This is in good agreement with the energy injection rate estimated in §4.2 and §4.3 to account for the radio flux from starbursts. This suggests that secondary electrons may dominate the radio emission in starbursts (see also Rengarajan 2005). If correct, it remains to be understood why normal spirals and starbursts lie on approximately the same FIR-radio correlation even though secondaries do not appear to be important for electrons emitting at $\sim \text{GHz}$ frequencies in normal spirals (Strong et al. 2004). As discussed in §4.2 variations in $\tau_{\text{syn}}/\tau_{\text{esc}}$ might also be expected to modify the FIR-radio correlation for normal spirals relative to starbursts.

4.5. Inverse Compton Emission

IC upscattering of infrared photons by cosmic-ray electrons can provide an independent constraint on U_B/U_{ph} because the ratio of the IC power to the radio power is given by $L_{\text{IC}}/L_{\text{rad}} \approx U_{\text{ph}}/U_B$. If we use equation (12) to estimate U_{ph} , then $B \sim B_{\text{eq}}$ in starbursts would lead to negligible IC power because it would imply $U_B/U_{\text{ph}} \gg 1$. However, if the infrared optical depth is larger than unity, equation (13) may instead be applicable, in which case $B \sim B_{\text{eq}}$ implies $U_B/U_{\text{ph}} \sim 1$.

IC emission has long been argued to contribute significantly to the X-ray emission in a variety of systems, including M82 (e.g., Hargrave 1974; Moran & Lehnert 1997) and NGC 3256 (e.g., Moran, Lehnert, & Helfand 1999). In both of these examples, however, much of the hard X-ray emission has been resolved into point sources with *Chandra*, although IC emission may still contribute to the hard X-rays from the very central nucleus of the starburst (e.g., Lira et al. 2002; Strickland et al. 2002; Strickland & Heckman, private communication). More detailed tests of this hypothesis would be very worthwhile given the possibility of providing an independent constraint on the magnetic field strength in starbursts.

4.6. Synchrotron Halos

As an alternative to the standard interpretation (§3.3) that extended synchrotron halos are due to relativistic electrons generated in the disk and advected into the halo (before cooling), we suggest that the halos are instead due to electrons accelerated *in situ* in the galactic wind, by either direct electron acceleration in shocks or via charged pion production. We note that in several simulations of galactic winds (e.g., Strickland & Stevens 2000), most of the X-ray emission is due to *in situ* shocks, which are also likely to be sites of particle acceleration. Since the total kinetic energy flux in a galactic wind is comparable to the energy produced by supernovae in the starburst, only a small fraction of the wind energy must be converted into relativistic particles *in situ* to account for the extended synchrotron emission observed. In this interpretation, which clearly requires additional work, $B \gg B_{\text{min}}$ would be fully consistent with extended synchrotron emission. Observed spectral differences between the galactic disk and halo in M82 and other systems may arise from spatial variations in $\tau_{\text{syn}}/\tau_{\text{esc}}$, $\tau_{\text{IC}}/\tau_{\text{esc}}$, $\tau_{\text{brem}}/\tau_{\text{syn}}$, and $\tau_{\text{ion}}/\tau_{\text{syn}}$.

5. DISCUSSION & CONCLUSIONS

Based on the analysis of the preceding sections, it is worthwhile contrasting the following two scenarios for the radio emission from starbursts:

$B \sim B_{\text{min}}$: For the minimum energy magnetic field estimate to be applicable, the electrons must escape rapidly in a galactic wind with $\tau_{\text{cool}} \gtrsim \tau_{\text{esc}}$. The rapid escape implies that there is no cooling break at GHz frequencies, which is consistent with the observed nonthermal spectra of $\alpha \approx 0.75$. Rapid escape is plausible given that hot outflowing galactic winds are observed from starbursts and that the cosmic rays are likely generated in the same supernova shocks that generate the wind. This interpretation of magnetic fields in starbursts — the standard one — has two major drawbacks: (1) it is difficult to see how $\tau_{\text{cool}} \gtrsim \tau_{\text{esc}}$ is applicable in ULIRGs where cooling times from IC alone are $\sim 10^4 \text{ yr}$ and (2) it is very difficult to account for the FIR-radio correlation with $\tau_{\text{cool}} \gtrsim \tau_{\text{esc}}$ because variations in τ_{cool} or τ_{esc} should lead to variations in the fraction of the electron energy radiated away via synchrotron radiation. Either several coincidences or a complex feedback loop are then required to account for the linearity of the FIR-radio correlation. The latter would be somewhat surprising given that B_{min} itself implies that magnetic fields and cosmic rays are dynamically weak compared to gravity (Fig. 1).

$B \gg B_{\text{min}}$: An alternative possibility is that magnetic fields in starbursts are much stronger than is suggested by the minimum energy estimate. Rapid cooling of relativistic electrons in starbursts will invalidate the minimum energy estimate if $\tau_{\text{cool}} \ll \tau_{\text{esc}}$. Magnetic fields in starbursts could then in principle be as large as $\sim B_{\text{eq}}$, which is ~ 10 times larger than B_{min} for typical starbursts (Fig. 1). This model naturally accounts for the linearity of the FIR-radio correlation because in the limit $\tau_{\text{cool}} \lesssim \tau_{\text{esc}}$ the radio flux is nearly independent of the magnetic field strength (e.g., Völk 1989). In addition, the observed radio luminosities from star-forming galaxies are comparable to the estimated rate at which energy is supplied to relativistic electrons in supernova shocks (§4.2). This supports the hypothesis that $\tau_{\text{cool}} \lesssim \tau_{\text{esc}}$. Independent support for this hypothesis is provided by the fact that the observed scaling $B_{\text{min}} \propto \Sigma_g^{2/5}$ for the minimum energy field in starbursts (Fig. 1) follows directly from the Schmidt Law for star formation when $\tau_{\text{cool}} \lesssim \tau_{\text{esc}}$ (eq. [10]).

A standard objection to $\tau_{\text{cool}} \lesssim \tau_{\text{esc}}$ is that the typical non-thermal spectral indices of starbursts ($\alpha \approx 0.75$) do not show the expected steepening due to strong cooling ($\alpha \approx 1$). We have argued, however, that if $B \gg B_{\text{min}}$ and if cosmic ray electrons interact with gas at approximately the mean density of the ISM, then ionization and bremsstrahlung losses flatten the radio spectra of starbursts at \sim GHz frequencies and reconcile $\tau_{\text{cool}} \lesssim \tau_{\text{esc}}$ with the observed spectra (Fig. 3). An important part of this argument is the realization that the ionization and bremsstrahlung loss times are similar to the synchrotron cooling time in all starburst galaxies for cosmic ray electrons emitting at GHz frequencies. Thus, ionization and bremsstrahlung losses can modify the nonthermal spectra of starburst galaxies and yet maintain the linearity of the FIR-radio correlation (Fig. 4).

This interpretation of magnetic fields in starbursts — that $B \gg B_{\text{min}}$ — has two potential drawbacks: (1) Given that galactic winds efficiently remove mass and metals from galaxies, it is unclear whether the cosmic rays actually interact with the bulk of the ISM in starbursts, which is required for ionization losses to be significant. (2) The nonthermal synchrotron halos observed in several systems are typically interpreted as cosmic-ray electrons advected out with a galactic wind, with synchrotron cooling only becoming important in the halo (e.g., Seaquist & Odegard 1991). If this interpretation is correct, it requires $B \sim B_{\text{min}}$ (§3.3). We have suggested, however, that extended synchrotron emission may be due to particles accelerated *in situ* in galactic winds (§4.6), in which case the observed halos cannot be readily used to constrain the magnetic field strength in galactic disks.

We believe that the arguments presented in this paper strongly favor $\tau_{\text{cool}} \lesssim \tau_{\text{esc}}$ for the relativistic electrons in starbursts. In this limit, the minimum energy argument underestimates the true magnetic field strength. The observed radio flux is, however, nearly independent of the magnetic field and depends primarily on the rate at which energy is supplied to relativistic electrons. Thus direct constraints on the true field strength are difficult to come by. By themselves, these arguments do not imply that $B \sim B_{\text{eq}}$, only that $\tau_{\text{cool}} \lesssim \tau_{\text{esc}}$ and $B \gtrsim B_{\text{min}}$. Our strongest argument that magnetic fields are likely to be $\gg B_{\text{min}}$ derives from the ratio of the ionization and bremsstrahlung loss times to the synchrotron cooling time: if cosmic ray electrons interact with gas having roughly the mean density of the ISM, magnetic fields *must* be $\gg B_{\text{min}}$ in starbursts in order for ionization and bremsstrahlung losses to not completely dominate over synchrotron losses (which would be inconsistent with the FIR-radio correlation and would require that an unreasonably large fraction of the supernova energy be supplied to cosmic ray electrons in order to account for the observed radio fluxes from starbursts; §4.3).

Our conjecture is thus that the magnetic field is significantly larger than $\sim B_{\text{min}}$ (the canonical estimate) in many starbursts. Confirming this prediction would have significant implications for understanding the physics of star formation in starbursts, the effects of magnetic fields on the dynamics of galactic winds, and the role of magnetic stresses in driv-

ing gas to smaller radii to fuel a central active galactic nucleus. Towards this end, we briefly summarize several observations that should help test the predictions of our model: (1) If ionization and bremsstrahlung losses are important, the radio spectra of starbursts should be flatter below ~ 1 GHz than they are above ~ 1 GHz (§4.3 and Fig. 3). (2) If cosmic rays interact with gas at about the mean density of the ISM, as is required for ionization and bremsstrahlung losses to be important, there should be an appreciable gamma-ray flux from starbursts due to neutral pion production (§4.4). We estimate $\nu L_{\nu} \approx 2 \times 10^{-5} L_{\text{IR}}$ above ≈ 100 MeV. This prediction is testable with *GLAST*. (3) Zeeman measurements of starbursts can directly probe the magnetic field strength in the dense phase of the ISM, and distinguish between $B \sim B_{\text{min}}$ and $B \gg B_{\text{min}}$. Existing upper limits in 4 ULIRGs from Killeen et al. (1996) are above B_{min} , but below the equipartition field (§3.1). (4) If $B \gg B_{\text{min}}$, IC emission is unlikely to contribute significantly to the X-ray emission in starbursts (§4.5).

It is interesting to compare our results on magnetic fields in starbursts with the inferred correlation between magnetic field strength, column density, and mass density in Galactic molecular clouds (e.g., Troland & Heiles 1986; Crutcher 1999). Using Zeeman splitting to determine the magnetic field strength directly, Crutcher (1999) finds that over the range $0.01 \text{ g cm}^{-2} \lesssim \Sigma_{\text{H}_2} \lesssim 2 \text{ g cm}^{-2} \lesssim$ and $2.7 \lesssim \log_{10}[n_{\text{H}_2} (\text{cm}^{-3})] \lesssim 6.8$, that $B \propto n_{\text{H}_2}^{1/2}$ and $B \propto \Sigma_{\text{H}_2}$. These findings imply both that the Alfvén speed $v_A \sim \text{constant} \sim 10 \text{ km s}^{-1}$ and that equipartition obtains. Observations of polarization in H_2O masers in dense star-forming regions provide evidence that these trends extend to yet higher densities ($10^8 - 10^{10} \text{ cm}^{-3}$; Sarma et al. 2002; Vlemmings et al. 2005). These results suggest that the magnetic field is always comparable to the total pressure in Galactic molecular clouds, with $B \approx B_{\text{eq}}$.

The sample of Galactic molecular clouds reviewed by Crutcher (1999) covers precisely the same surface densities represented by starbursts in our Figure 1. It is thus particularly striking that the minimum energy estimate implies $B \ll B_{\text{eq}}$ in starbursts, while direct Zeeman measurements of local molecular clouds with the same Σ_g imply $B \sim B_{\text{eq}}$. Our suggestion is that this difference arises in part from the inapplicability of the minimum energy estimate in starbursts.

We are grateful to Rainer Beck, Tim Heckman, and Jim Condon for a close reading of the text and for a number of very useful comments. We also thank Alberto Bolatto, Bruce Partridge, and Carl Heiles for valuable conversations. E.Q. is supported in part by NASA grant ATP05-54, an Alfred P. Sloan Fellowship, and the David and Lucile Packard Foundation. E.W. thanks the Miller Foundation for supporting his visit to UC Berkeley and the Institute for Advanced Study. N.M. is supported in part by a Canadian Research Chair in Astrophysics. This research made extensive use of the NASA Extragalactic Database. C.L.M. is supported by the David and Lucile Packard foundation and Alfred P. Sloan Fellowship.

REFERENCES

- Aharonian, F., et al. 2005, *A&A*, 437, L7
 Allen, R. J., Sancisi, R., & Baldwin, J. E. 1978, *A&A*, 62, 397
 Beck, R. 2000, *Phil Trans. R. Soc. London, Ser. A*, 358, 777
 Beck, R. 2001, *Space Science Reviews*, 99, 243
 Beck, R., & Krause, M. 2005, *Astronomical Notes*, 326, 414
 Becker, R. H., White, R. L., & Edwards, A. L. 1991, *ApJS*, 75, 1
 Bell, E. F. 2003, *ApJ*, 586, 794
 Beuermann, K., Kanbach, G., & Berkhuijsen, E. M. 1985, *A&A*, 153, 17

- Boulares, A., & Cox, D. P. 1990, *ApJ*, 365, 544
- Blandford, R., & Eichler, D. 1987, *Phys. Rep.*, 154, 1
- Bressan, A., Silva, L., & Granato, G. L. 2002, *A&A*, 392, 377
- Brogan, C. L., Gaensler, B. M., Gelfand, J. D., Lazendic, J. S., Lazio, T. J. W., Kassim, N. E., & McClure-Griffiths, N. M. 2005, *ApJ*, 629, L105
- Burbidge, G. R. 1956, *ApJ*, 124, 416
- Carilli, C. L., Holdaway, M., Ho, P., & de Pree, C. G. 1992, *ApJ*, 399, L59
- Chevalier, R. A., & Clegg, A. W. 1985, *Nature*, 317, 44
- Cillis, A. N., Torres, D. F., & Reimer, O. 2005, *ApJ*, 621, 139
- Condon, J. J. 1987, *ApJS*, 65, 485
- Condon, J. J., Yin, Q. F., & Burstein, D. 1987, *ApJS*, 65, 543
- Condon, J. J., & Broderick, J. J. 1988, *AJ*, 96, 30
- Condon, J. J., Helou, G., Sanders, D. B., & Soifer, B. T. 1990, *ApJS*, 73, 359
- Condon, J. J., Frayer, D. T., & Broderick, J. J. 1991, *AJ*, 101, 362
- Condon, J. J., Huang, Z.-P., Yin, Q. F., & Thuan, T. X. 1991, *ApJ*, 378, 65
- Condon, J. J. 1992, *ARA&A*, 30, 575
- Condon, J. J., Helou, G., Sanders, D. B., & Soifer, B. T. 1996, *ApJS*, 103, 81
- Condon, J. J., Cotton, W. D., Greisen, E. W., Yin, Q. F., Perley, R. A., Taylor, G. B., & Broderick, J. J. 1998, *AJ*, 115, 1693
- Connell, J. J. 1998, *ApJ*, 501, L59
- Crutcher, R. M. 1999, *ApJ*, 520, 706
- Dahlem, M., Petr, M. G., Lehnert, M. D., Heckman, T. M., & Ehle, M. 1997, *A&A*, 320, 731
- de Vaucouleurs, G., de Vaucouleurs, A., & Corwin, H. G. 1976, *Second Reference Catalog of Bright Galaxies (Austin: Univ. Texas Press) (RC2)*
- Downes, D., & Solomon, P. M. 1998, *ApJ*, 507, 615
- Dumke, M., & Krause, M. 1998, *LNP Vol. 506: IAU Colloq. 166: The Local Bubble and Beyond*, 506, 555
- Duric, N. 1990, *IAU Symp. 140: Galactic & Intergalactic Magnetic Fields*, 140, 235
- Ekers, R. D., & Sancisi, R. 1977, *A&A*, 54, 973
- Ficarra, A., Grueff, G., & Tomassetti, G. 1985, *A&AS*, 59, 255
- Fish, V. L., Reid, M. J., Argon, A. L., & Menten, K. M. 2003, *ApJ*, 596, 328
- Fitt, A. J., & Alexander, P. 1993, *MNRAS*, 261, 445
- Garcia-Munoz, M., Mason, G. M., & Simpson, J. A. 1977, *ApJ*, 217, 859
- Griffith, M. R., Wright, A., Burke, B., & Ekers, R. D. 1995, *ApJS*, 97, 347
- Hales, S. E. G., Baldwin, J. E., & Warner, P. J. 1993, *MNRAS*, 263, 25
- Hargrave, P. J. 1974, *MNRAS*, 168, 491
- Heeschen, D. S., & Wade, C. M. 1964, *AJ*, 69, 277
- Helou, G., Soifer, B. T., & Rowan-Robinson, M. 1985, *ApJ*, 298, L7
- Hummel, E. 1980, *A&AS*, 41, 151
- Hummel, E., Dahlem, M., van der Hulst, J. M., & Sukumar, S. 1991, *A&A*, 246, 10
- Irwin, J. A., & Saikia, D. J. 2003, *MNRAS*, 346, 977
- Israel, F. P., & de Bruyn, A. G. 1988, *A&A*, 198, 109
- Israel, F. P., & Mahoney, M. J. 1990, *ApJ*, 352, 30
- Kennicutt, R. C. 1998, *ApJ*, 498, 541
- Keshet, U., Waxman, E., Loeb, A., Springel, V., & Hernquist, L. 2003, *ApJ*, 585, 128
- Killeen, N. E. B., Staveley-Smith, L., Wilson, W. E., & Sault, R. J. 1996, *MNRAS*, 280, 1143
- Klein, U., Wielebinski, R., & Morsi, H. W. 1988, *A&A*, 190, 41
- Kuehr, H., Witzel, A., Pauliny-Toth, I., & Nauber, U. 1981, *A&AS*, 45, 367
- Large, M. I., Mills, B. Y., Little, A. G., Crawford, D. F., & Sutton, J. M. 1981, *MNRAS*, 194, 693
- Lira, P., Ward, M., Zezas, A., Alonso-Herrero, A., & Ueno, S. 2002, *MNRAS*, 330, 259
- Lisenfeld, U., Wilding, T. W., Pooley, G. G., & Alexander, P. 2004, *MNRAS*, 349, 1335
- Longair, M. S. 1994, *High Energy Astrophysics, Vol. II Second Edition (Cambridge: Cambridge University Press)*
- Martin, C. L. 1999, *ApJ*, 513, 156
- Moran, E. C., & Lehnert, M. D. 1997, *ApJ*, 478, 172
- Moran, E. C., Lehnert, M. D., & Helfand, D. J. 1999, *ApJ*, 526, 649
- McCutcheon, W. H. 1973, *AJ*, 78, 18
- Niklas, S. 1995, *Ph.D. Thesis*
- Niklas, S., Klein, U., & Wielebinski, R. 1997, *A&A*, 322, 19
- Oly, C., & Israel, F. P. 1993, *A&AS*, 100, 263
- Parker, E. N. 1965, *ApJ*, 142, 584
- Parker, E. N. 1966, *ApJ*, 145, 811
- Rengarajan, T. N. 2005, *Proceedings of the 29th International Cosmic Rays Conference, Pune, India, astro-ph/0511156*
- Sarma, A. P., Troland, T. H., Crutcher, R. M., & Roberts, D. A. 2002, *ApJ*, 580, 928
- Scoville, N. Z., Yun, M. S., & Bryant, P. M. 1997, *ApJ*, 484, 702
- Seaquist, E. R., & Odegard, N. 1991, *ApJ*, 369, 320
- Strickland, D. K., & Stevens, I. R. 2000, *MNRAS*, 314, 511
- Strickland, D. K., Heckman, T. M., Weaver, K. A., Hoopes, C. G., & Dahlem, M. 2002, *ApJ*, 568, 689
- Strong, A. W., Moskalenko, I. V., & Reimer, O. 2000, *ApJ*, 537, 763
- Strong, A. W., Moskalenko, I. V., & Reimer, O. 2004, *ApJ*, 613, 962
- Thompson, T. A., Quataert, E., & Murray, N. 2005, *ApJ*, 630, 167
- Torres, D. F., 2004, *ApJ*, 617, 966
- Troland, T. H., & Heiles, C. 1986, *ApJ*, 301, 339
- Vallee, J. P. 1995, *A&A*, 296, 819
- van der Kruit, P. C. 1971, *A&A*, 15, 110
- van der Kruit, P. C. 1973, *A&A*, 29, 263
- Vlemmings, W., Diamond, P., van Langevelde, H., & Torrelles, J. 2005, *accepted to A&A, astro-ph/0510452*
- Voelk, H. J. 1989, *A&A*, 218, 67
- Waldrum, E. M., Yates, J. A., Riley, J. M., & Warner, P. J. 1996, *MNRAS*, 282, 779
- Yun, M. S., Reddy, N. A., & Condon, J. J. 2001, *ApJ*, 554, 803

TABLE 1
PROPERTIES OF NORMAL STAR-FORMING GALAXIES

Object Name	z^a	D^b (Mpc)	$\log_{10}[\Sigma_g]^{c,d}$ (g cm^{-2})	$\log_{10}[\dot{\Sigma}_*]^{e,d}$ ($M_\odot \text{ yr}^{-1} \text{ kpc}^{-2}$)	$S_{1.4\text{GHz}}^f$ (mJy)	$\log_{10}[L_{\text{rad}}]^g$ (W Hz^{-1})	Angular Diameter ^d ($''$)	Radius (kpc)	B_{min}^h (μG)	B_{eq}^i (μG)	Radio Data References
NGC 224.....	...	0.9	-3.00	-3.13	8400	20.89	9912	20.9	3.3	2.3	1
NGC 598.....	...	0.9	-2.65	-2.47	3300	20.51	3354	7.3	4.6	5.1	1
NGC 628.....	0.0022	9.3	-2.75	-2.18	180	21.27	612	13.8	5.3	4.1	1
NGC 772.....	0.0082	34.6	-2.74	-2.84	71.4	22.01	432	36.3	5.0	4.2	1
NGC 925.....	...	9.3	-2.77	-2.44	46.0	20.68	534	12.0	3.9	3.9	1
NGC 1569.....	...	2.2	-2.35	-0.80	411	20.40	150	0.82	15.1	10.2	1
NGC 2336.....	0.0074	31.1	-2.77	-1.92	17.7	21.31	414	31.2	3.4	3.9	1
NGC 2403.....	...	3.3	-2.80	-2.15	330	20.64	948	7.6	4.9	3.6	1
NGC 2841.....	0.0021	9.0	-2.71	-2.99	83.8	20.91	408	8.9	5.4	4.5	1
NGC 2903.....	...	6.1	-2.82	-2.31	407	21.26	642	9.5	6.5	3.5	1
NGC 2976.....	...	3.4	-2.70	-1.66	50.8	19.85	294	2.4	5.6	4.6	1
NGC 3031.....	...	3.3	-2.83	-2.50	380	20.70	1332	10.6	4.2	3.4	1
NGC 3310.....	0.0033	13.9	-2.54	-1.14	383	21.95	210	7.1	12.2	6.6	1
NGC 3338.....	0.0043	18.3	-2.87	-2.56	28.1	21.06	354	15.7	4.3	3.1	1
NGC 3368.....	0.0030	12.6	-2.75	-2.55	30.0	20.76	390	12.0	4.1	4.1	1
NGC 3486.....	0.0023	9.6	-2.80	-2.46	59.4	20.82	426	9.9	4.8	3.6	1
NGC 3521.....	0.0027	11.3	-2.46	-1.91	357	21.74	486	13.4	7.4	7.9	1
NGC 3631.....	0.0039	16.3	-2.52	-1.73	80.8	21.41	276	10.9	6.7	6.9	1
NGC 3675.....	0.0026	10.8	-2.69	-2.01	43.7	20.79	354	9.3	4.9	4.7	1
NGC 3726.....	0.0028	12.0	-2.62	-2.28	27.4	20.68	324	9.4	4.5	5.5	1
NGC 3893.....	0.0032	13.7	-2.62	-1.96	134	21.48	234	7.8	8.5	5.5	1
NGC 3938.....	0.0027	11.4	-2.48	-2.11	61.7	20.99	318	8.8	5.7	7.6	1
NGC 4178.....	0.0013	5.3	-2.55	-2.27	23.3	19.90	240	3.1	5.1	6.4	1
NGC 4254.....	0.0080	33.9	-2.29	-1.70	422	22.77	312	25.7	10.0	11.7	1
NGC 4258.....	0.0015	6.3	-3.09	-2.36	790	21.58	906	13.9	6.5	1.9	1
NGC 4294.....	0.0012	5.0	-2.66	-1.87	24.9	19.88	150	1.8	6.8	5.0	2
NGC 4303.....	0.0052	22.1	-2.47	-1.74	416	22.39	354	19.0	9.2	7.7	1
NGC 4321.....	0.0053	22.4	-2.54	-2.07	340	22.31	408	22.1	8.1	6.6	1
NGC 4394.....	0.0031	13.0	-3.04	-2.88	0.7	19.15	234	7.4	1.9	2.1	1
NGC 4402.....	0.0008	3.3	-2.60	-2.80	52.2	19.85	186	1.5	7.4	5.7	3
NGC 4501.....	0.0076	32.1	-2.59	-2.21	278	22.54	360	28.0	8.2	5.9	1
NGC 4519.....	0.0041	17.2	-2.69	-1.98	9.1	20.51	186	7.8	4.5	4.7	2
NGC 4535.....	0.0065	27.6	-2.67	-2.38	64.5	21.77	378	25.3	5.2	4.9	1
NGC 4548.....	0.0016	6.8	-2.99	-2.52	4.6	19.42	306	5.1	2.8	2.3	1
NGC 4569.....	...	18.0	-3.07	-2.78	83.4	21.51	474	20.7	4.9	1.9	1
NGC 4571.....	...	15.0	-2.85	-2.56	4.2	20.06	222	8.1	3.2	3.2	1
NGC 4579.....	0.0051	21.4	-2.87	-2.32	103	21.76	306	15.9	6.7	3.1	1
NGC 4647.....	0.0047	19.9	-2.64	-2.22	35.0	21.23	204	9.9	6.2	5.2	3
NGC 4651.....	0.0028	12.0	-2.62	-1.98	24.0	20.62	210	6.1	5.5	5.5	1
NGC 4654.....	0.0035	14.6	-2.58	-2.06	117	21.48	258	9.1	7.7	6.0	1
NGC 4689.....	0.0054	22.8	-2.74	-2.38	9.6	20.78	234	12.9	4.0	4.2	1
NGC 4698.....	0.0033	14.1	-3.43	-3.55	0.6	19.16	222	7.6	1.9	0.8	1
NGC 4713.....	0.0022	9.2	-2.64	-1.53	37.8	20.59	156	3.5	7.4	5.2	2
NGC 4736.....	0.0010	4.4	-3.03	-2.22	254	20.78	630	6.8	5.8	2.1	1
NGC 4826.....	0.0014	5.8	-3.01	-2.47	103	20.61	480	6.7	5.2	2.2	1
NGC 5033.....	0.0029	12.4	-2.75	-2.64	178	21.52	546	16.4	5.7	4.1	1
NGC 5055.....	0.0017	7.1	-2.51	-2.32	390	21.38	660	11.4	6.4	7.1	1
NGC 5194.....	0.0015	6.5	-2.21	-1.78	1490	21.88	600	9.4	9.8	14.1	1
NGC 5236.....	0.0017	7.3	-1.98	-1.41	2445	22.19	660	11.6	10.7	23.9	1
NGC 5457.....	...	8.0	-2.59	-2.46	750	21.77	1614	31.4	4.6	5.9	1
NGC 6217.....	0.0045	19.2	-2.39	-1.91	78.4	21.54	180	8.4	8.4	9.3	1
NGC 6503.....	...	5.2	-2.79	-2.08	36.5	20.08	294	3.7	5.1	3.7	1
NGC 6643.....	0.0049	20.9	-2.57	-1.81	92.2	21.69	204	10.3	8.2	6.2	1
NGC 6946.....	...	3.0	-2.38	-1.88	1395	21.17	642	4.6	9.3	9.5	1
NGC 7331.....	0.0027	11.6	-2.60	-2.33	373	21.78	510	14.3	7.3	5.7	1

REFERENCES. — (1) Condon (1987); (2) Condon, Yin, & Burstein (1987); (3) Condon et al. (1990).

^aRedshifts from NED. ^bDistance. In most cases, distances are computed from z with $H = 71 \text{ km s}^{-1} \text{ Mpc}^{-1}$. In cases where redshifts are not a reliable distance indicator, D is taken from the literature. ^cGas surface density. ^dData from Kennicutt (1998). ^eStar formation rate per unit area. ^fRadio flux density listed at 1.4 and 1.49 GHz. ^gRadio luminosity computed using $L_{\text{rad}} = 4\pi D^2 S_{1.4\text{GHz}}$. ^h B_{min} calculated using equation (1), with $\nu_{\text{GHz}} = 1.49$, $V = 2\pi R^2 h_{\text{rad}}$, and assuming $h_{\text{rad}} = 500 \text{ pc}$. ⁱ B_{eq} calculated using equation (3).

TABLE 2
PROPERTIES OF STARBURST GALAXIES

Object Name	z^a	D^b (Mpc)	$\log_{10}[\Sigma_g]^c$ (g cm^{-2})	$\log_{10}[\dot{\Sigma}_*]^d$ ($M_\odot \text{ yr}^{-1} \text{ kpc}^{-2}$)	$S_{1.4\text{GHz}}^f$ (mJy)	$\log_{10}[L_{\text{rad}}]^g$ (W Hz^{-1})	Angular Diameter ^d ($''$)	Radius (kpc)	B_{min}^h (mG)	B_{eq}^i (mG)	Radio Data References
NGC 253.....	...	3.5	-0.33	1.24	5594	21.93	24	0.21	0.14	1.1	1
NGC 520.....	0.0074	31.2	0.13	1.32	167	22.29	5	0.38	0.13	3.1	2
NGC 660.....	0.0028	12.0	-1.08	0.06	387	21.83	31	0.90	0.06	0.19	2
NGC 828.....	0.0179	75.7	-0.02	1.10	108	22.87	5	0.92	0.11	2.2	3
NGC 891.....	0.0018	7.4	-1.07	-0.58	701	21.67	35	0.63	0.06	0.19	3
NGC 1097.....	0.0043	18.0	-1.01	-0.20	415	22.21	35	1.52	0.05	0.22	3
NGC 1614.....	0.0159	67.3	0.04	1.79	123	22.83	4	0.65	0.13	2.5	2
NGC 1808.....	0.0034	14.2	-1.03	0.08	519	22.10	30	1.03	0.06	0.21	1
NGC 2146.....	0.0030	12.6	-0.85	0.84	1087	22.32	17	0.52	0.11	0.32	1
NGC 2623.....	0.0185	78.0	-0.81	1.00	98.5	22.86	8	1.51	0.08	0.35	2
NGC 3034 (M82).....	...	3.3	-0.16	1.48	7657	22.00	29	0.23	0.14	1.6	2
NGC 3079.....	0.0038	15.9	0.57	1.63	849	22.41	5	0.19	0.20	8.5	2
NGC 3351.....	0.0026	11.0	-0.85	0.24	47.8	20.84	14	0.37	0.05	0.32	2
NGC 3504.....	0.0051	21.7	-0.78	0.11	265	22.18	16	0.84	0.08	0.38	2
NGC 3627.....	0.0024	10.2	-1.40	-0.77	458	21.76	39	0.97	0.05	0.09	2
NGC 3690.....	0.0100	42.2	-1.40	-0.10	658	23.15	24	2.46	0.08	0.09	2
NGC 6240.....	0.0243	102.7	0.43	1.87	392	23.70	3	0.75	0.22	6.2	3
NGC 7552.....	0.0053	22.3	-1.30	0.16	276	22.22	22	1.19	0.06	0.11	1
IC 342.....	0.0010	4.4	-1.62	-0.41	2250	21.71	67	0.71	0.06	0.05	1
IC 694.....	0.0104	43.8	0.42	2.40	153	22.55	2.6	0.28	0.18	6.0	4
IC 883 (Arp 193).....	0.0233	98.5	0.27	1.54	101	23.07	3.4	0.81	0.14	4.26	2
IC 1623.....	0.0204	86.1	0.13	1.67	221	23.30	3.6	0.75	0.17	3.1	2
Maffei 2.....	...	3.0	-1.22	-0.27	286	20.48	40	0.29	0.05	0.14	5
Arp 55.....	0.0393	165.9	-0.95	0.32	33	23.04	8	3.22	0.06	0.26	6
Arp 220.....	0.0181	76.6	1.08	2.98	324	23.36	2	0.37	0.26	27.5	2
IRAS 10173+0828.....	0.0480	202.8	-1.27	0.48	9.9	22.69	7	3.44	0.05	0.12	6
IRAS 17208-0014.....	0.0425	179.4	0.41	2.01	73	23.45	3	1.30	0.14	5.9	6
VII Zw 31.....	0.0537	226.8	-0.57	0.82	41.6	23.41	5	2.75	0.09	0.62	3
Zw 049.057.....	0.0332	140.1	0.22	1.77	46.4	23.04	3	1.02	0.12	3.8	2

REFERENCES. — (1) Condon (1987); (2) Condon et al. (1990); (3) Condon et al. (1996); (4) Condon & Broderick (1988); (5) Condon et al. (1998); (6) Yun, Reddy, & Condon (2001).

^aRedshifts from NED. ^bDistance. In most cases, distances computed with $H = 71 \text{ km s}^{-1} \text{ Mpc}^{-1}$. In some cases, distances are taken from the literature instead of using the Hubble Law. ^cGas surface density. ^dData taken from Kennicutt (1998). ^eStar formation rate per unit area. ^fRadio flux density listed at 1.40, 1.425, or 1.49 GHz. ^gRadio luminosity computed using $L_{\text{rad}} = 4\pi D^2 S_{1.4\text{GHz}}$. ^h B_{min} calculated using equation (1), with $\nu_{\text{GHz}} = 1.49$, $V = 2\pi R^2 h_{\text{rad}}$, and assuming $h_{\text{rad}} = 100 \text{ pc}$. ⁱ B_{eq} calculated using equation (3).

TABLE 3
PROPERTIES OF “EXTREME” STARBURST GALAXIES

Object Name	z^a	D^b (Mpc)	$\log_{10}[\Sigma_g]^c$ (g cm^{-2})	$\log_{10}[\dot{\Sigma}_*]^d$ ($M_\odot \text{ yr}^{-1} \text{ kpc}^{-2}$)	$S_{8.44\text{GHz}}^e$ (mJy)	$\log_{10}[L_{\text{rad}}]^f$ (W Hz^{-1})	Angular Diameter ^c ($''$)	Radius (kpc)	B_{min}^g (mG)	B_{eq}^h (mG)	Radio Data References
IC 883 (Arp 193).....	0.0233	98.5	0.25	2.68	34.9	22.61	0.69	0.16	0.33	4.06	1
Mrk 273.....	0.0378	159.6	0.66	3.36	43.5	23.13	0.35	0.14	0.51	10.45	1
Arp 220 (west).....	0.0181	76.6	0.94	3.55	72.2	22.71	0.40	0.07	0.55	19.91	1
Arp 220 (east).....	0.0181	76.6	0.78	2.96	60.7	22.63	0.66	0.12	0.39	13.77	1

REFERENCES. — (1) Condon et al. (1991).

^aRedshifts from NED. ^bDistances computed with $H = 71 \text{ km s}^{-1} \text{ Mpc}^{-1}$. ^cGas surface density from Downes & Solomon (1998), Tables 3, 4, and 12. Values adjusted for assumed H_0 . ^dStar formation rate per unit area computed using $\dot{\Sigma}_* = L_{\text{IR}}(< R)/(\pi R^2 \epsilon c^2)$ with $\epsilon = 3.8 \times 10^{-4}$ (see Downes & Solomon 1998 Table 12). ^eRadio flux density at 8.44 GHz. ^fRadio luminosity computed using $L_{\text{rad}} = 4\pi D^2 S_{8.44\text{GHz}}$. ^g B_{min} calculated using equation (1), with $\nu_{\text{GHz}} = 8.44$, $V = 2\pi R^2 h_{\text{rad}}$, and assuming $h_{\text{rad}} = 100 \text{ pc}$. ^h B_{eq} calculated using equation (3).